RESEARCH ARTICLE doi.org/10.1002/adsc.202301285

Advanced Synthesis & Catalysis

Asymmetric Boracarboxylation of Styrenes Using Carbon Dioxide

Martin Pettersen,[+a] Cuong Dat Do,[+a, b] Sai Manoj N. V. T. Gorantla,[a, b] Marc F. Obst,[a] Roman Damm,[a] Anggi E. Putra,[a] Ashot Gevorgyan,[a] Ljiljana Pavlovic,[a] Kathrin H. Hopmann,[+a,*] and Annette Bayer[+a,*]

[a] Department of Chemistry, UiT The Arctic University of Norway, N-9017 Tromsø, Norway
E-mail: annette.bayer@uit.no; kathrin.hopmann@uit.no
[b] Hylleraas Center for Quantum Molecular Sciences, UiT The Arctic University of Norway, N-9017 Tromsø, Norway

[+] Have contributed equally.

Manuscript received: November 6, 2023; Revised manuscript received: April 16, 2024;
Version of record online: May 29, 2024

Supporting information for this article is available on the WWW under https://doi.org/10.1002/adsc.202301285

Abstract: The boracarboxylation reaction has potential for the production of natural products and drug candidates, but the development of an asymmetric version of this transformation is challenging. We report an enantioselective boracarboxylation of styrenes, enabled by a copper catalyst containing chiral phosphines. Our experimental conditions provide yields between 31–76% and enantiomeric ratios from 80:20 up to 98:2 for electron-rich styrenes. Oxidation of a boracarboxylation product gives (*S*)-tropic acid, an intermediate towards several tropane alkaloids. A computational analysis of the mechanistic details shows a complex pattern of competing reaction pathways, highlighting challenges encountered when developing asymmetric reactions using CO_2.

Keywords: Asymmetric catalysis; Carbon dioxide fixation; Carboxylation; Copper; Computational chemistry; Reaction mechanism

Introduction

Carbon dioxide is a cheap and widely abundant waste gas that can serve as a source of carbon. One of its possible applications is as a building block for the formation of value-added chemicals.[1] This requires efficient ways to form C–C bonds with CO_2. The use of CO_2 in carboxylation reactions is of large interest, given the abundance of carboxylic acid functional groups in natural and medicinal compounds.[2] A review from 2020 concluded that over 60% of all bioactive molecules described in the medicinal chemistry literature contain at least one carboxylic acid moiety or another functional group that can be derived from a carboxylic acid.[3]

Conventional methods for carboxylation using CO_2, such as the Grignard reaction and the Kolbe-Schmitt reaction, are well developed, have been commercialized and can be used to prepare food additives such as benzoic and acetic acid or pharmaceutical products such as salicylic acid.[4] In the last two decades, there has been increasing focus on developing catalytic and electrochemical methods for CO_2-based carboxylations, broadening the scope of CO_2-based chemical transformations.[5]

The ability to form chiral carboxylic acids plays a critical role in natural product synthesis and drug development. However, the number of catalytic asymmetric carboxylations employing CO_2 is limited.[6] In 2004, the Mori group demonstrated the generation of three stereocenters through Ni-catalysed carboxylative cyclization of bis-1,3-dienes with an enantiomeric ratio (*e.r.*) up to 96:4 and yields up to 99%.[7] A notable study was published in 2016 by Mikami's group, who

applied a chiral Rh-based catalyst in the hydrocarboxylation of acrylates. In their study, an *e.r.* of up to 83:17 was achieved, at moderate yields (14-69%).[8] Another significant study in the field of asymmetric CO_2 utilization was published by the group of Yu in 2017.[9] They reported a Cu-catalyzed hydroxymethylation of styrenes and 1,3-dienes, achieved from an in-situ reduction of the intermediate carboxylate, obtaining excellent *e.r.* values (up to 99:1) and yields (up to 96%). Later, this method was extended to the hydroxymethylation of 1,1-disubstituted-1,3-dienes[10] and 1,1-disubstituted allenes[11] producing quarternary stereocentres with good enantioselectivity.

Also in 2017, Marek and co-workers achieved a Cu-catalysed asymmetric carbomagnesiation of cyclopropene using CO_2 as electrophile in one example. The reaction exhibited good yields (up to 75%) and excellent *e.r.* values (up to 98:2).[12] Recently, enantioselective carbo-carboxylations of alkenes via a Ni-catalysed Heck coupling/carboxylation cascade have been reported by the groups of Lopez and Bandini,[13] and Kong and Yu.[14] The first example of an enantioselective electrochemical carboxylation was reported by Lu and co-workers in 2009 transforming acetophenone to the corresponding α-hydroxy acid with an *e.r.* of 65:35.[15] Recently, the method was modified to provide an *e.r.* of up to 97:3 for selected examples.[16] The group of Lu also reported the electrochemical transformation of benzylic halides to the corresponding carboxylic acids with an *e.r.* up to 92:8 using either a chiral homogeneous[17] or heterogeneous[18] co-catalyst. Similarly, in 2018, Mei and co-workers reported the electrochemical carboxylation of allylic acetates, with an *e.r.* of up to 84:16 using a chiral Pd-catalyst.[19]

One reaction of interest in terms of asymmetric development is the boracarboxylation, which allows for direct carboxylation of an unsaturated C–C bond using CO_2 as a carbon source. The simultaneous addition of a boron moiety creates a reactive C–B bond that subsequently can be used for derivatization via transformations such as oxygenation, amination and homologation. The first reported catalytic boracarboxylation of unsaturated C–C bond dates from 2012. Hou and co-workers (Scheme 1a) described the boracarboxylation of various alkynes using carbon dioxide and bis(pinacolato)diboron (B_2pin_2), in the presence of an NHC-copper(I)-based catalyst.[20] Popp and co-workers showed that similar reaction conditions could also be used for the regioselective boracarboxylation of substituted styrenes (Scheme 1b),[21] as well as α-substituted vinyl arenes.[22] During the review process for this article, two related asymmetric carboxylations were published. Gui, Yu and coworkers described an asymmetric Cu-catalysed 1,4-dicarboxylation of 1,3-dienes proceeding via a boracarboxylation intermediate with an *e.r.* of >99:1.[23] The group of

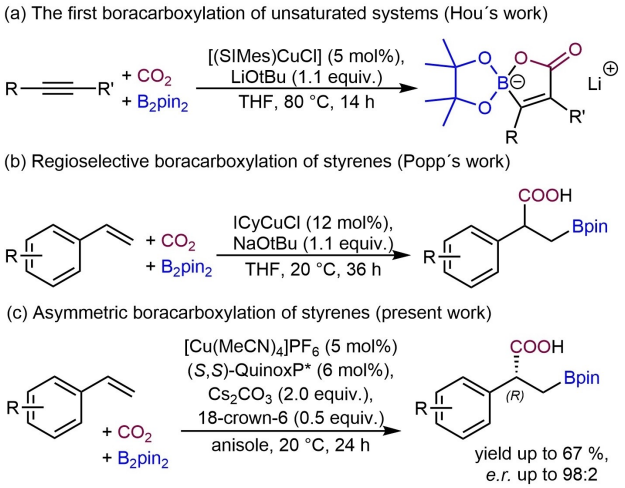

Scheme 1. Previously reported boracarboxylations of a) acetylenes,[20] and b) styrenes,[21c] and c) the present work on stereoselective boracarboxylation.

Zhou and Tang reported a Cu-catalysed boracarboxylation of styrenes using a chiral NHC–Cu catalyst providing excellent enantioselectivities up to *e.r.* >98:2 for electron-rich substrates.[24]

Computational analyses of the regioselective boracarboxylation of unsaturated substrates[25] have indicated a plausible reaction pathway, with elementary steps involving i) formation of the reactive copper(I) boronate species, ii) insertion of the unsaturated substrate into the copper-boron bond, and iii) carboxylation at the carbon bound to copper (Scheme 2).

Here, we present our work towards an asymmetric boracarboxylation method allowing for the enantioselective addition of CO_2 to styrenes, with good yields and enantioselectivity (Scheme 1c). Furthermore, a chiral boracarboxylation product was selectively trans-

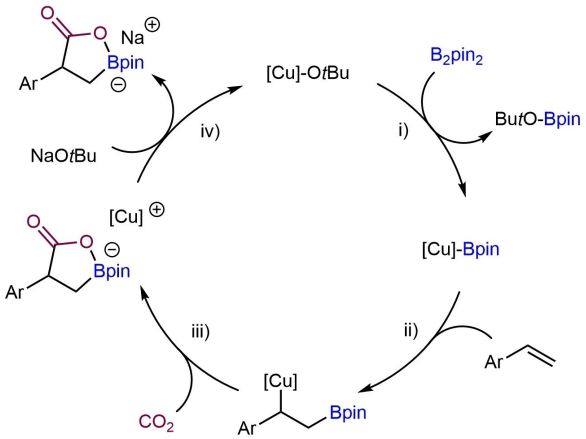

Scheme 2. Proposed mechanism for the copper-catalyzed boracarboxylation of styrenes.[20,22,25–26]

formed to tropic acid, a precursor for several natural products and drugs, demonstrating the utility of the reaction and determining the absolute configuration of the product. Detailed computational studies of the reaction mechanism reveal multiple competing carboxylation pathways, which impact the enantioselective outcome.

Results and Discussion

Our investigation commenced with the development of a regioselective boracarboxylation protocol based on phosphine ligands. Our preliminary studies showed that phosphine-based copper catalysts can be very effective for boracarboxylation of styrenes (SI, **Table S1–S3**). In particular the combination of $[Cu(MeCN)_4]PF_6$ and (*S,S*)-BDPP in the presence of Cs_2CO_3 as a base in 2-MeTHF leads to formation of the boracarboxylation product of 4-methylstyrene in 84% isolated yield, albeit with a close to racemic result (*e.r.* 48:52, Table 1, entry 1).

Based on the initial reaction conditions, we investigated a range of commercially available chiral phosphine ligands (Table 1 and complete overview in SI, **Table S4**). In addition, some chiral NHC-ligands were included in the screening (Table 1, entry 7 and 8).[21c,22] Relative to the results obtained for (*S,S*)-BDPP (84% yield), the yields of the reaction dropped for other chiral phosphines. The next best phosphine ligands in terms of yield (44-46%) were (*R,R,R,R*)-BIBOP, (*R*)-Walphos and (*3S,3'S*)-BABIBOP (entry 2–4). At this stage, (*3S,3'S*)-BABIBOP (entry 4) showed the best enantioselectivity (*e.r.* 23:77), with similar enantiomeric ratios obtained for the well-known ligands (*R*)-BINAP (*e.r.* 30:70; entry 5) and (S_{Fc},R_c)-Mandyphos (*e.r.* 23:77; entry 6). The chiral NHC-ligands L1 and L2 (entry 7–8) showed good yields (71% and 72%), but low selectivities (L1 *e.r.* 35:65 and L2 *e.r.* 48:52). The promising results obtained for (*3S,3'S*)-BABIBOP prompted us to extend our study towards other *P*-chiral phosphines, such as (*R,R*)-BenzP* (entry 9) and (*S,S*)-QuinoxP* (entry 10).[27] While both resulted in poor yields (23-26%), (*S,S*)-QuinoxP* (entry 10) exhibited an excellent enantioselectivity, providing the boracarboxylation product with an *e.r.* of 92:8. With these results in hand, we proceeded to optimize reaction conditions using (*S,S*)-QuinoxP* as chiral ligand.

Initially, we focused on altering the solvent. Although ethers did not provide better results, somewhat improved yields of 40% were obtained with anisole (Table 2, entry 2), which could be increased to 76% yield by doubling the catalyst loading to 10 mol% (Table 2, entry 8). This reaction showed a good enantiomeric ratio of 84:16. A change of the base to alkoxides such as NaO*t*Bu, which worked well for carbene ligands,[21c] did not improve yields (Table 2, entry 4). The copper source had critical impact on the yield, with a change in counterion resulting in a drop to 18–26% (Table 2, entry 5–7). Inclusion of different additives such as phase transfer catalysts and weakly coordinating anions did not provide any improvement (Table 2, entry 12–15), apart from 18-crown-6 ether (Table 2, entry 9), which demonstrated a significant enhancement from 40% to 58% yield at 5 mol% catalyst loading. The addition of 18-crown-6 did not only increase the yield, but also slightly improved the enantioselectivity from *e.r.* 92:8 to 96:4. Increased catalyst loading with 18-crown-6 as an additive did not result in further improvement (Table 2, entry 10). Performing the reaction at −20 °C further increased the

Table 1. The performance of selected chiral phosphines for the boracarboxylation of 4-methylstyrene (**1 a**).

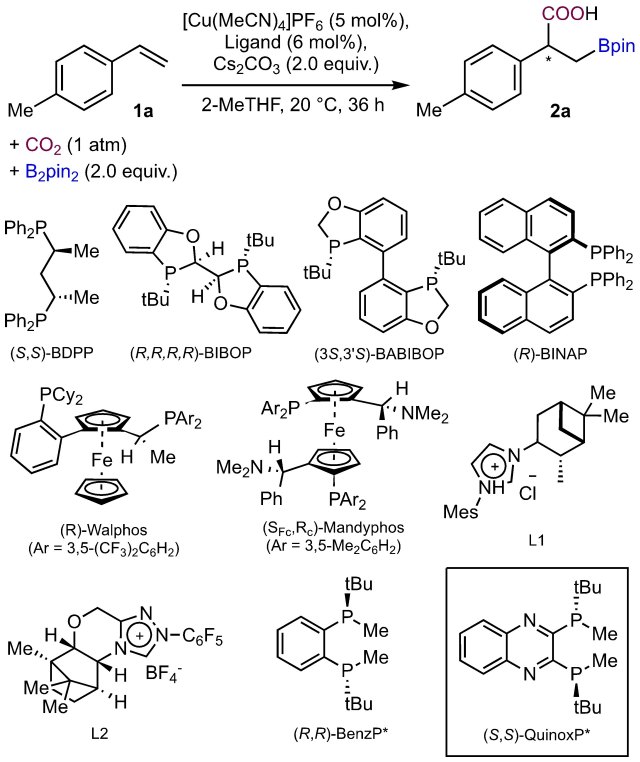

Entry	Ligand	*e.r.*[a]	Yield[b]
1	(*S,S*)-BDPP	48:52	84%
2	(*R,R,R,R*)-BIBOP	43:57	46%
3	(*R*)-Walphos	39:61	44%
4	(*3S,3'S*)-BABIBOP	23:77	45%
5	(*R*)-BINAP	30:70	22%
6	(S_{Fc},R_c)-Mandyphos	23:77	20%
7	L1	35:65	71%
8	L2	48:52	72%
9	(*R,R*)-BenzP*	23:77	23%
10	(*S,S*)-QuinoxP*	92:8	26%

[a] The enantiomeric ratio of the product was determined by super critical fluid chromatography with a chiral column.
[b] Isolated yields.

Table 2. Summary of the optimization of the reaction for (*S,S)*-QuinoxP* (n.d. = not determined).

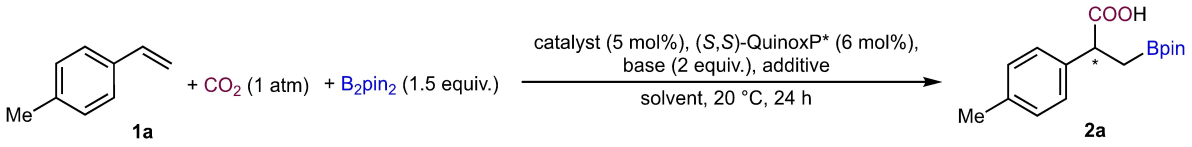

Entry	Cu source	Base	Additive (mol%)	Solvent	*e.r.*	Yield[a]
1	$[Cu(MeCN)_4]PF_6$	Cs_2CO_3	–	Dioxane	n.d.	25%
2	$[Cu(MeCN)_4]PF_6$	Cs_2CO_3	–	Anisole	92:8	40%
3	$[Cu(MeCN)_4]PF_6$	Cs_2CO_3	–	Triglyme	n.d.	19%
4	$[Cu(MeCN)_4]PF_6$	NaO*t*Bu	–	Anisole	n.d.	26%
5	$[Cu(MeCN)_4]BF_4$	Cs_2CO_3	–	Anisole	n.d.	18%
6	$[Cu(MeCN)_4]SbF_6$	Cs_2CO_3	–	Anisole	n.d.	20%
7	$[Cu(MeCN)_4]$BarF	Cs_2CO_3	–	Anisole	n.d.	26%
8	$[Cu(MeCN)_4]PF_6$	Cs_2CO_3	–	Anisole	84:16	76%[b]
9	$[Cu(MeCN)_4]PF_6$	Cs_2CO_3	18-crown-6 (50)	Anisole	96:4	66%
10	$[Cu(MeCN)_4]PF_6$	Cs_2CO_3	18-crown-6 (50)	Anisole	93:7	60%[b]
11	$[Cu(MeCN)_4]PF_6$	Cs_2CO_3	18-crown-6 (50)	Anisole	>99:1	11%[c]
12	$[Cu(MeCN)_4]PF_6$	Cs_2CO_3	TBAB (50)	Anisole	95:5	42%
13	$[Cu(MeCN)_4]PF_6$	Cs_2CO_3	PPh_3 (20)	Anisole	91:9	32%
14	$[Cu(MeCN)_4]PF_6$	Cs_2CO_3	monolaurin (20)	Anisole	87:13	37%
15	$[Cu(MeCN)_4]PF_6$	Cs_2CO_3	palmitic acid (20)	Anisole	94:6	33%

[a] Isolated yields.
[b] 10 mol% of Cu-source and 12 mol% of the ligand was used.
[c] Reaction at −20 °C.

enantioselectivity to an excellent *e.r.* of >99:1, however at the cost of the isolated yield (Table 2, entry 11).

We moved on to study the reaction for a range of electron-rich, electron-deficient, and electron-neutral styrenes (Scheme 3) using $[Cu(MeCN)_4]PF_6$/(*S,S)*-QuinoxP* as precatalyst, Cs_2CO_3 as base combined with 18-crown-6 as additive in anisole as solvent. Styrenes with a methyl substituent in para, meta or ortho position (**1a**, **1d** and **1g**) could be selectively functionalized in 37–66% yields with enantiomeric ratios ranging from good (82:18) to excellent (96:4).

In general, electron-rich substrates **1a**–**1h** gave good enantioselectivities (>80:20), except for the sterically more demanding substrates **1i**–**1l** where the enantioselectivity went down. The yields were fair (33-42%). Investigating the mass balance for the boracarboxylation of **1a** and **1d** (SI, **Spectrum S55**–**S56**), we observed the formation of borylated styrenes corresponding to a competing β-hydride elimination instead of a carboxylation pathway accounting for 23% and 30%, respectively. In both reactions, the boracarboxylation and β-hydride elimination products accounted for ~75% of the styrene starting material.

Electron-withdrawing substituents such as fluorine (**1m** and **1p**), trifluoromethyl (**1n** and **1q**), cyano (**1o**), nitro (**1s**) and ester (**1t**) resulted in comparable yields to those seen for electron-neutral and -rich systems (13-67%). Except for **1m** (*e.r.* 89:11), low enantiomeric ratios were observed for electron-deficient substrates. Racemisation due to basic reaction conditions was eliminated as a cause for the low *e.r.* by stirring products **2a**, **2p** and **2q** for 24 h under reaction conditions but without catalyst precursors, showing no change in *e.r.* We therefore hypothesised that electronic effects from the substrate impact the enantioselectivity of boracarboxylations. This hypothesis was investigated by adding a fluorine to the electron-rich substrates **1e** and **1h**, which resulted in a noticeable drop in *e.r.* for the products **2f** and **2r**. We note that reduced enantioselectivities are commonly reported for additions of Cu–H and Cu-Bpin complexes to electron-deficient alkenes.[28] A mechanistic study by Hoveyda and coworkers suggested that reduced enantioselectivity is caused by the formation of a non-chiral Cu-alkyl intermediate formed upon ligand loss and showed that increased ligand concentration improved the selectivity.[28] However, for the boracarboxylation of **1n** an increased ligand concentration (from 6 to 12 mol%) did not influence the enantioselectivity.

We also explored the potential impact of the CO_2 pressure on the enantioselectivity of the reaction. In a recent study, the Popp group showed that higher pressures of CO_2 can benefit the yield of the reactions involving electron-deficient systems.[22] Accordingly, we investigated the influence of the CO_2 pressure on the yield and enantioselectivity for electron-deficient substrates (**1m**, **1n**, **1p** and **1q**). While the yields for the reactions involving these substrates increased for products **2m** (from <5% to 19%), **2n** (from 38% to

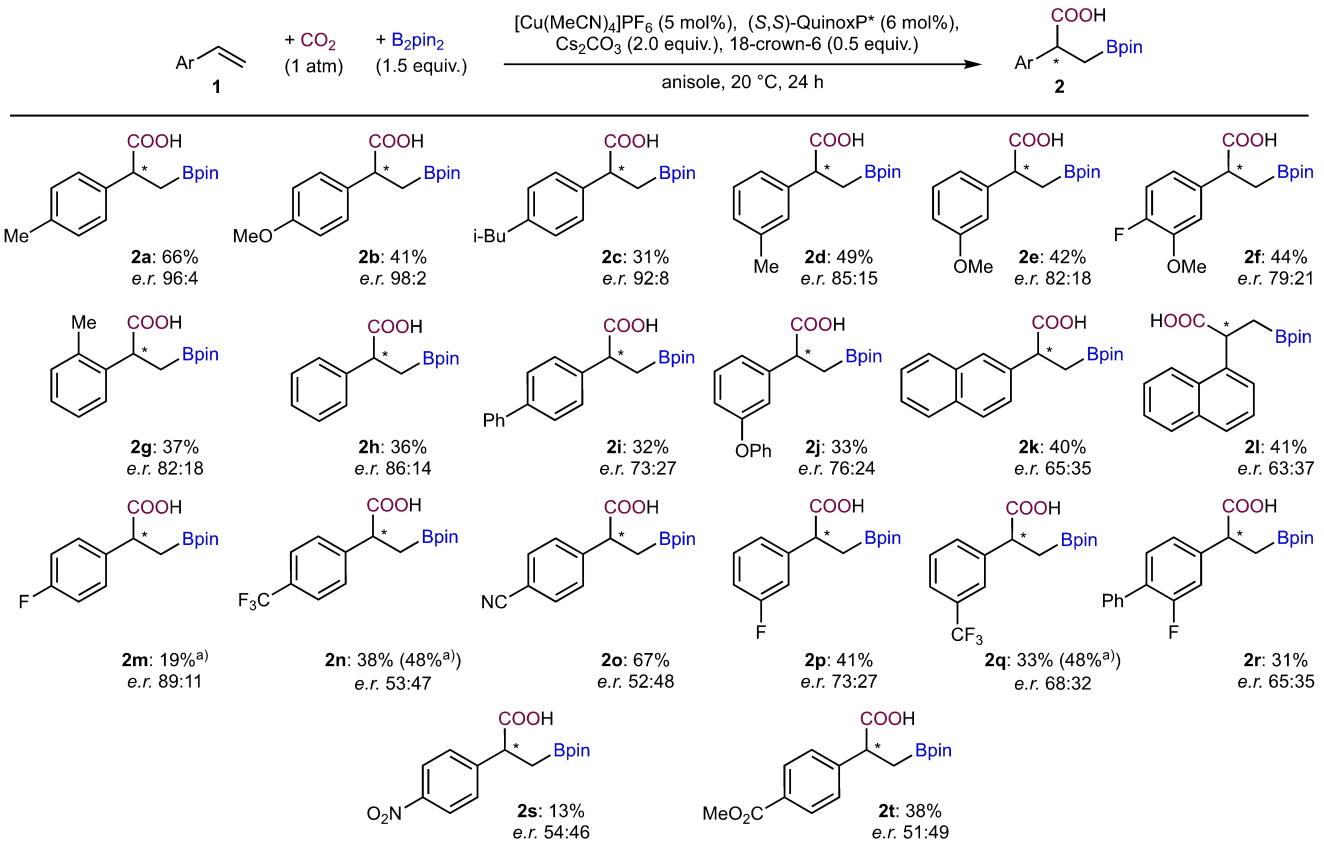

Scheme 3. The substrate scope of the asymmetric boracarboxylation with isolated yields and enantiomeric ratios *(e.r.)*. [a] Yield obtained at 5 atm of CO_2.

48%) and **2q** (from 33% to 48%), the enantiomeric ratio was practically unaffected.

To establish the absolute configuration of the major boracarboxylation product, we employed sodium perborate tetrahydrate to convert **2h** to tropic acid **3h** (Scheme 4). The later was obtained in a quantitative yield, with the enantiomeric ratio of the product retained (SI, **Chromatogram S21**). Comparing tropic acid **3h** with commercial (*R*)-tropic acid as reference, we established that the (*R*)-enantiomer of **2h** was formed upon boracarboxylation of **1h** with (*S,S*)-QuinoxP. The transformation of (*R*)-**2h** to (*S*)-tropic acid **3h** also demonstrates the formal total synthesis of the natural product (*S*)-scopolamine,[29] and the anticholineric drugs (*S*)-oxitropium (Oxivent)[30] and (*S*)-tropicamide (Mydriacyl)[31] via a boracarboxylation (Scheme 4).

A computational analysis of the mechanistic details was performed, initially focusing on substrate **1a** and the (*S,S*)-BDPP ligand (SI, Figures S10–S11 and Table S10). The most relevant reaction pathways (see Scheme 5) were then studied with (*S,S*)-QuinoxP*. We hypothesized that the first step of the reaction would be the formation of the reactive copper borate **A** through the activation of B_2pin_2 with the base Cs_2CO_3,[32] and the subsequent transmetallation be-

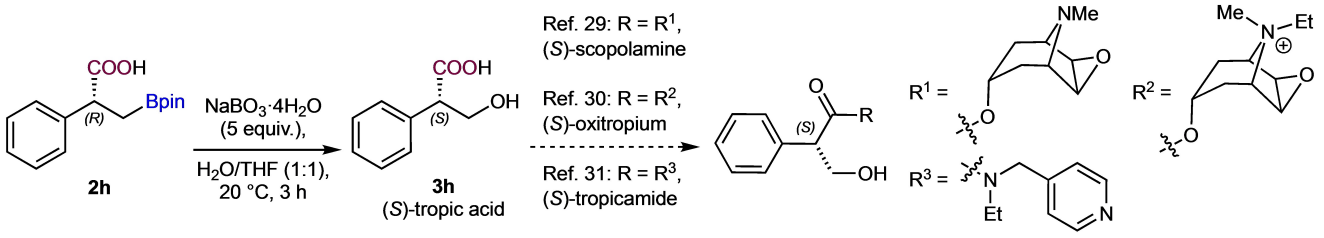

Scheme 4. Transformation of (*R*)-**2h** to (*S*)-tropic acid **3h**, a synthetic intermediate towards bioactive tropic acid esters and amides.

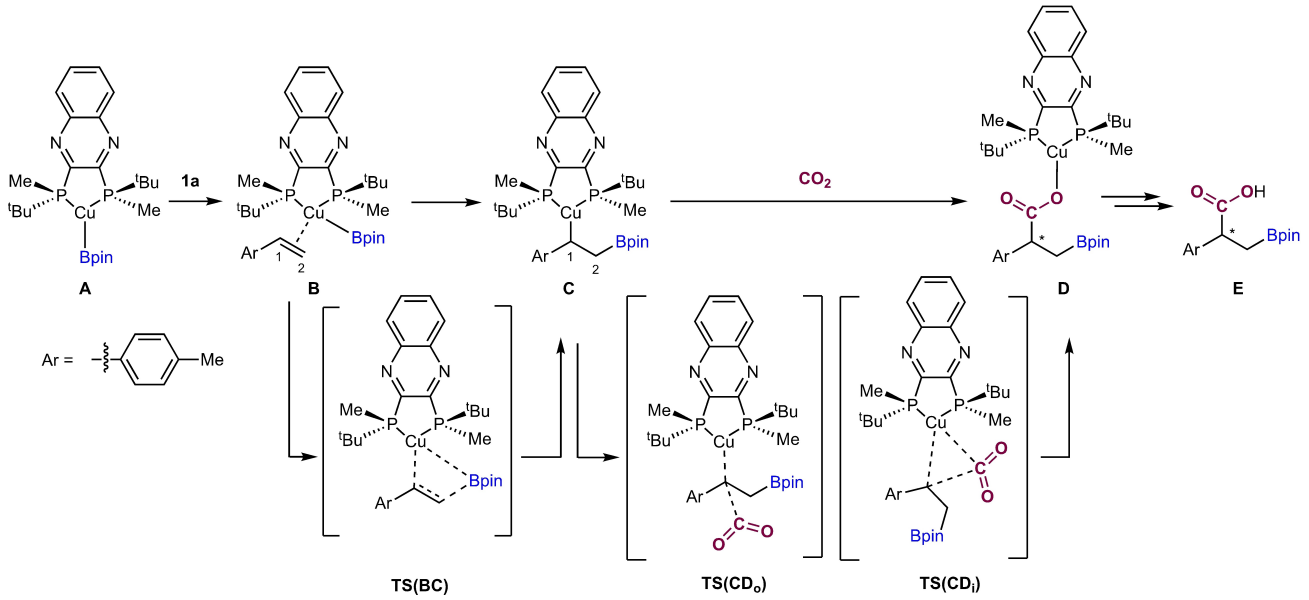

Scheme 5. Proposed mechanism for the boracarboxylation of styrene **1 a**.

tween the activated diboron species and the copper complex (see SI, Scheme S1 for details). Coordination of styrene **1 a** to **A** leads to formation of intermediate **B**, followed by a 2,1-boracupration to form the borylated intermediate **C** (Scheme 5 and Figure 1). The latter step involves the transfer of the borate to the terminal position of the substrate, which in our calculations has a low barrier (2.3 to 3.3 kcal/mol relative to **B**, depending on the resulting stereoisomer. The computed TSs were confirmed through IRC calculations. We note that reported barriers for boracupration are functional dependent (SI, Figures S14–S15), with values of 10.5 to 31.1 kcal/mol reported in the literature.[25a,28,33] The alternative 1,2-boracupration displays a higher insertion barrier (12.4 kcal/mol relative to **B**, ESI, Figure S12), explaining the absence of the corresponding product in our experiments.

The formed intermediate **C** exists as two diastereomeric forms ($\mathbf{C}_R$ and $\mathbf{C}_S$) with either (*R*) or (*S*) configuration at the benzylic carbon. The formation of $\mathbf{C}_R$ and $\mathbf{C}_S$ is exergonic by 15.2 and 16.5 kcal/mol, respectively, relative to **A** (Figure 1). Considering that the reverse barriers from **C** to **B** are less than 20 kcal/

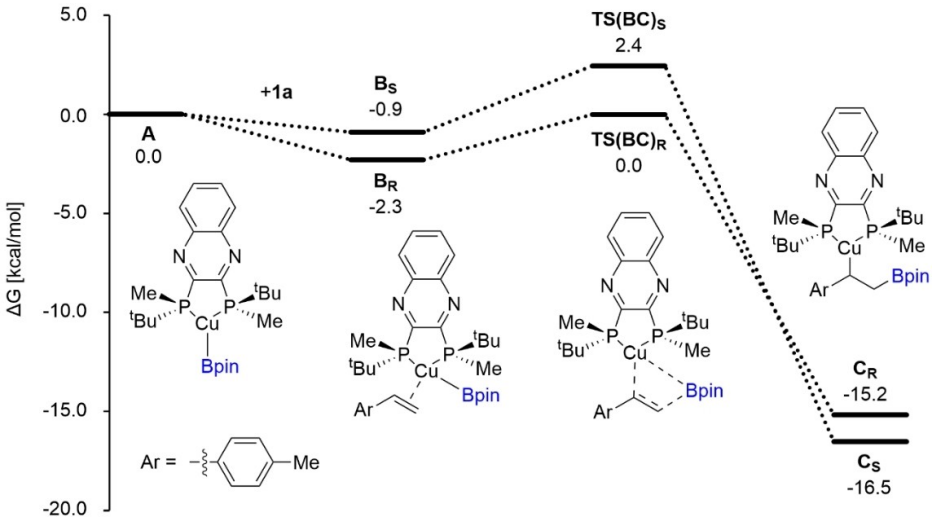

Figure 1. Gibbs free energy profile (kcal/mol, PBE-D3BJ/pc-2//PBE-D3BJ/6-31 + G*(SDD for Cu), IEFPCM:THF, 298.15 K) for the QunioxP*-Cu-mediated formation of intermediate **C** from **1 a**.

mol at room temperature (Figure 1),[34] it can be assumed that the diastereomeric species can interconvert, which would imply Curtin Hammett conditions.[35] However, we note that different functionals provide a slightly different description of the energetics: while PBE-D3BJ and PBE0-D3BJ support a reversible borylation of **1a** (Figure 1 and SI, Figures S13–S14), optimizations with M06 indicate that the reverse step from **C** to **B** would have a barrier of ~26 kcal/mol, making it less likely (SI, Figure S15). Thus, the reversibility of the boracupration step cannot be established conclusively (*vide infra*).

The subsequent CO_2 insertion into the diastereomeric intermediates $\mathbf{C}_R$ and $\mathbf{C}_S$ may occur through either an inner or outer sphere CO_2 insertion. We have previously shown that the preferred pathway is determined by the substrate type and the size of the ligand.[36] For enantioselective reactions, it is important to highlight that if CO_2 insertion occurs in an inner sphere fashion (where CO_2 interacts with the Cu centre), the configuration at the benzylic carbon in **C** is retained, whereas outer sphere insertion (where CO_2 does not interact with Cu) results in an inversion. Consequently, both $\mathbf{C}_R$ and $\mathbf{C}_S$ can independently form the carboxylated product species $\mathbf{D}_R$ and $\mathbf{D}_S$.

Starting from $\mathbf{C}_S$, the computed outer sphere carboxylation TS has a barrier of 13.7 kcal/mol, which is significantly lower than the inner sphere TS (17.4 kcal/mol, Figure 2). From $\mathbf{C}_R$, both outer and inner sphere pathways have near-identical barriers (~14 kcal/mol relative to $\mathbf{C}_R$, Figure 2). This highlights that there is no clear preference for inner versus outer sphere carboxylation of benzylic carbons with QuinoxP*-Cu as catalyst and both pathways can be expected to occur. The reverse barriers from **D** to **C** are higher than 40 kcal/mol (Figure 2), which indicates that CO_2 insertion is irreversible at room temperature. The overall thermodynamic driving force for the formation of the free boracarboxylated products from **1a** was computed to −67.3 kcal/mol.

The optimized geometries of the CO_2 insertion TSs (Figure 3) show that the CO_2 molecule is stabilized by C–H/O interactions with the substrate. In the inner sphere TSs, a significant distortion of the substrate occurs to accommodate the CO_2 molecule, which interacts with both the benzylic carbon and the copper atom. In the outer sphere TSs, the CO_2 molecule approaches the substrate from the backside of the $C_{(benzylic)}$–Cu bond, with CO_2 showing significantly less bending (O–C–O angles ~156°) compared to the inner sphere TSs (O–C–O angles ~137°). Looking specifically at the lowest energy conformation, $\mathbf{TS(CD_o)}_{S\rightarrow R}$, a C–H/O interaction (2.50 Å) between the ligand and one of the Bpin oxygens stabilizes this conformation compared to $\mathbf{TS(CD_o)}_{R\rightarrow S}$ (closest analogous interaction is 3.47 Å). Also the C–H/π interactions between ligand and substrate are significantly stronger at **TS-**

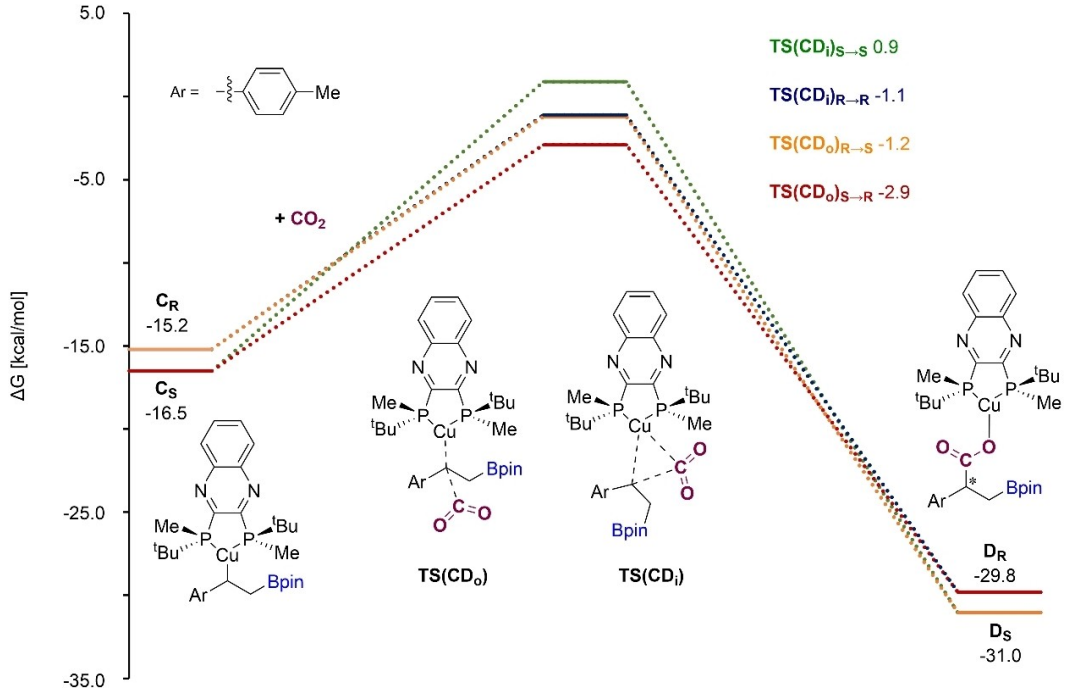

Figure 2. Gibbs free energy profile for the insertion of CO_2 into the diastereomeric **C** intermediates (kcal/mol, PBE-D3BJ/pc-2//PBE-D3BJ/6-31+G*(SDD for Cu), IEFPCM:THF, 298.15 K, energies are given relative to **A**). TS(CD_i) refers to inner sphere TSs, and TS(CD_o) refers to outer sphere TSs.

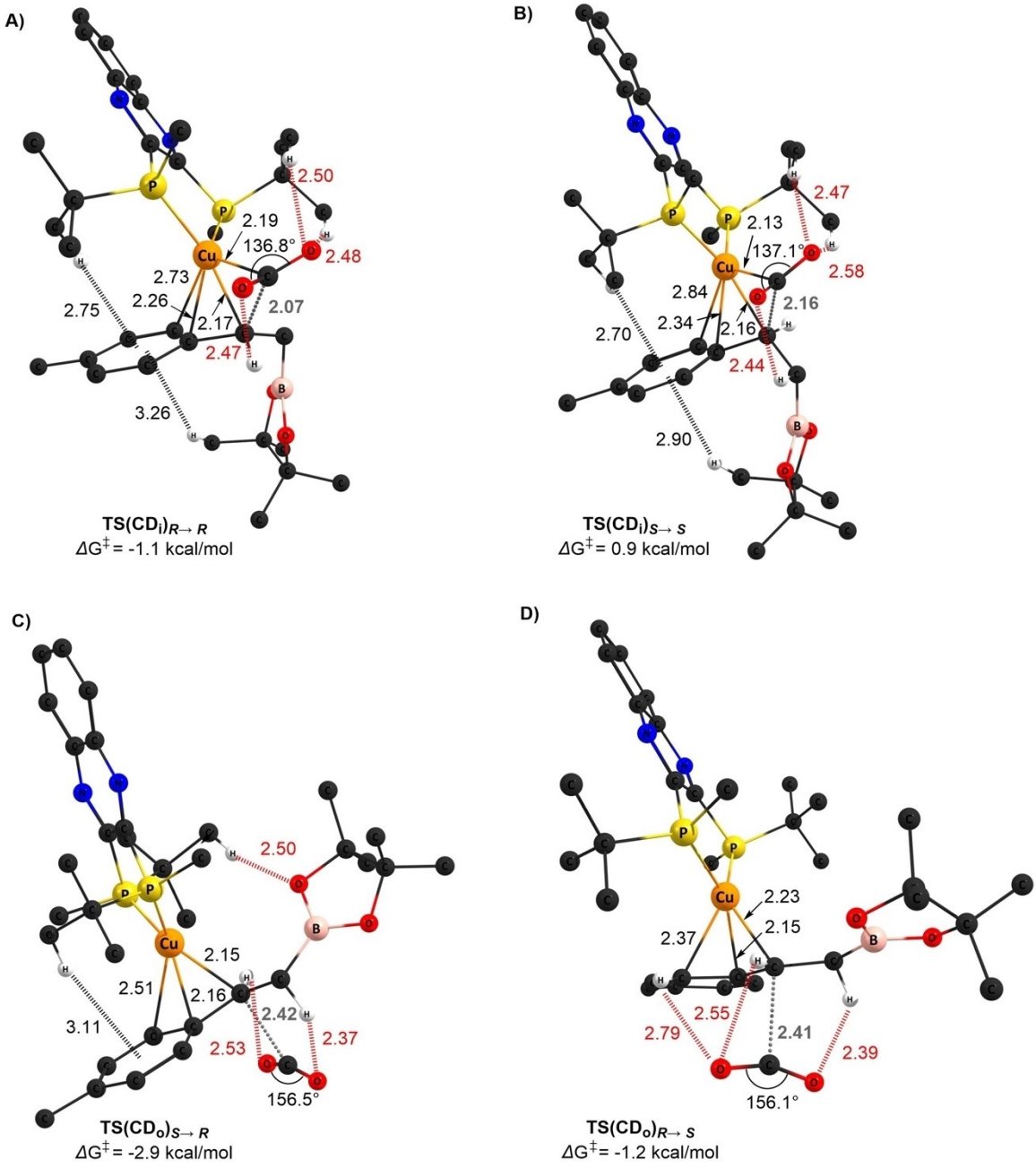

Figure 3. Optimized geometries of all four CO_2 insertion TSs, grey = C–C(CO_2) distances, red = attractive C–H/O interactions, black = attractive C–H/π interactions, distances in Å. Note that energies are relative to **A**, PBE-D3BJ/pc-2//PBE-D3BJ/6-31 + G*(SDD for Cu), IEFPCM:THF, 298.15 K. For clarity, only hydrogen atoms of interest are shown.

$(CD_o)_{S\rightarrow R}$ (down to ~2.7 Å), compared to **$TS(CD_o)_{R\rightarrow S}$** (~3.2 Å, coordinates for all geometries are given in the SI).

The enantioselectivity of the final reaction will depend on the relative barriers for CO_2 insertion, as well as on the reversibility of the boracurpation step. We note that the backwards barriers (**C** to **B**, Figure 1) are slightly higher than the forward CO_2 barriers (**C** to **D**, Figure 2). For example, **C_R** to **B** has a computed barrier of 15.2 kcal/mol (Figure 1), compared to 14.0 for **C_R** to **D** (Figure 2). This trend is also seen for other tested functionals (SI, Figures S13–S15) and may indicate that **C** is more likely to be carboxylated than to revert back to **B**. However, it is important to take into account that the methodological approximations made in computing the *intramolecular* boracupration step (**B** to **C**) and the *bimolecular* CO_2 insertion (**C** to **D**) are quite different; thus these barriers cannot be compared directly, as their relative errors may be several kcal/mol different.[37]

On basis of the computed results, we propose that there are two possible scenarios regarding the fate of intermediate **C**: The most likely scenario is that the diastereomeric intermediates $\mathbf{C}_R$ and $\mathbf{C}_S$ are able to interconvert (this is supported by feasible backwards barriers computed with most computational protocols, PBE-D3BJ[THF], PBE-D3BJ[anisole], PBE0-D3BJ[anisole]; Figure 1 and SI, Figure S13–S14). Under such circumstances, the *e.r.* of the final product will only depend on the barriers of the energetically available CO_2 insertion pathways.[35b] On the basis of the four TSs leading to **D** (Figure 2), we obtain a theoretical *e.r.* of 95:5 (298 K, PBE-D3BJ, THF) in favour of the (*R*)-product, which is in excellent agreement with the experimentally observed *e.r.* of 92:8 to 96:4 (Table 1, entry 10 and Table 2, entries 2 and 9). Other computational protocols provide very similar results (PBE-D3BJ[anisole]: 92:8, PBE0-D3BJ[anisole]: 93:7; SI, Table S12, Figures S13–S14). Interestingly, the effects of temperature on the computed barriers reproduce the experimental trend, with increasing *e.r.* as the temperature goes down (SI, Table S13).

The second scenario is that the formation of intermediate **C** is not reversible. As stated above, the energetics with M06 indicate that the reverse step from **C** to **B** has a relatively high barrier (~26 kcal/mol, SI, Figure S15). Thus, M06 predicts that mostly $\mathbf{C}_R$ will be formed and carboxylated, with a preference for an inner sphere TS, leading to a predicted *e.r.* of 97:3 (SI, Figure S15), again in excellent agreement with the experimental selectivity. This result highlights that high enantioselectivity can be obtained for this reaction also in the absence of Curtin-Hammett conditions. Further experimental analysis is recommended to evaluate the reversibility of the boracupration step.

As discussed above, when examining the crude reaction mixtures of the boracarboxylation of **1a**, we see 23% of borated styrene (SI, Spectrum S55), possibly formed through a competing β-hydride-elimination from **C**, in line with previous results.[21c] We calculated the β-hydride elimination pathway using (*S,S*)-QuinoxP* as ligand, which shows a barrier of 17.1 kcal/mol (SI, Scheme S2), thus being 3.4 kcal/mol higher than the lowest CO_2 insertion step (13.7 kcal/mol, Figure 2). This energy difference rationalizes the formation of small amounts of borated styrene in experiments.

Conclusion

We have developed a boracarboxylation method for the enantioselective addition of CO_2 to styrenes, using a chiral copper catalyst derived from the *P*-chiral ligand (*S,S*)-QuinoxP* and $[Cu(MeCN)_4]PF_6$. Our approach provides the boracarboxylation product with high regioselectivity and yields between 31–76%. The enantioselectivity of the reaction clearly depends on the electronic structure of the styrene, with electron-rich styrenes providing the best enantiomeric ratios >80:20. Detailed computational studies of the mechanism show that the reaction occurs through multiple competing pathways, which impacts the enantioselective outcome. For the studied copper precatalysts based on phosphine ligands, we find that inner and outer sphere carboxylations show similar barriers, indicating that both pathways will compete. This phenomenon significantly impacts the enantioselectivity and complicates the development of a robust enantioselective method. Nonetheless, our synthetic protocol provides enantiomeric ratios of up to 98:2, which are comparable to the best enantioselectivities reported so far for CO_2-based carboxylations. The chiral β-boronated carboxylic acids accessible in this way provide valuable building blocks for the synthesis of natural products and pharmaceuticals as shown by the synthesis of (*S*)-tropic acid, an intermediate in the synthesis of some tropane alkaloids and drugs derived thereof.

Experimental Section

Synthetic details: Commercially available starting materials, reagents, catalysts, ligands, solvents, and anhydrous solvents were used without further purification. The chiral ligands were purchased from Sigma Aldrich and Stream chemicals. Racemates were prepared according to the literature procedure.[21c] Non-anhydrous solvents were dried using activated 4 Å molecular sieves. ^1H, ^{13}C and ^{19}F NMR spectra were recorded on a Bruker Avance 400 MHz at 20 °C. All ^1H NMR spectra were reported in parts per million (ppm) downfield of TMS and were measured relative to the signals for residual $CHCl_3$ (7.26 ppm). All ^{13}C NMR spectra were reported in ppm relative to residual $CDCl_3$ (77.20 ppm) and were obtained with ^1H decoupling. Coupling constants, J, were reported in Hertz (Hz). High-resolution mass spectra (HRMS) were recorded from methanol solutions on an LTQ Orbitrap XL (Thermo Scientific) either in negative or in positive electrospray ionization (ESI) mode. Infrared spectra were recorded on an Agilent Cary 630 FT-IR spectrometer and absorptions are reported in wavenumber (cm^{-1}); br = broad, s = strong, m = medium, w = weak. Melting points were recorded using Stuart SMP50 automatic melting point detector. Optical rotation measurements were performed using a Polarimeter AA-10R from Optical Activity LTD. Determination of *e.r.* values were carried out on a Waters ACQUITY UPC2 system equipped with a Trefoil™ AMY1, 2.5 µm 3.0 x 150 mm column. Compounds were detected on a Waters ACQUITY PDA detector spanning wavelengths from 190 to 400 nm. The resolution of the products was performed with a mobile phase consisting of supercritical CO_2 and *i*-PrOH containing 0.5% of TFA and a linear gradient of 2–20% *i*-PrOH over 8 min followed by isocratic 1.5 min of 20% *i*-PrOH with a flow rate of 1.0 mL/min (SFC method A) or a linear gradient of 2–30% *i*-PrOH over 8 min followed by isocratic 1.5 min of 30% *i*-PrOH with a flow rate of 1.5 mL/min (SFC method B).

Representative Procedure for the Asymmetric Boracarboxylation

An oven dried 100 mL round bottom flask (see **Figure S1**) and a stir bar were introduced to the argon filled glove box. To the round bottom flask, a magnetic stir bar, B_2pin_2 (1.5 equiv.), base (2.0 equiv.), ligand (6 mol%) and Cu-salt (5 mol%) were added, closed with a septum, and sealed tight using electric tape. To the flask, 20 mL of solvent were added and left stirring for 30 minutes. Then the corresponding styrene (1 equiv.) was added, and a balloon filled with dry CO_2 was attached to the flask. The round bottom flask was then left stirring for 24 hours at 20° C (see **Figure S5**). Afterwards, the flask was opened to air and the content was diluted with 20 mL of Et_2O. The reaction mixture was transferred into a 250 mL separating funnel where the organic layer was extracted using a solution of saturated $NaHCO_3$ (3x30 mL). Then the separated aqueous solution was first washed with Et_2O (3x30 mL), acidified by slow addition of 60 mL 6 M HCl and then extracted using Et_2O (3x30 mL). The organic solution was washed using 30 mL of distilled water. Afterwards the organic solution was evaporated to dryness to give the product.

Computational Details

All molecules were calculated without truncations or symmetry constraints, using the Gaussian 16 program, revision B.01.[38] Geometries were optimized at the PBE[39] level of theory with the 6–31 + G* basis set[40] (using the SDD ECP for Cu), including the D3BJ dispersion correction by Grimme.[41] The solvation effects were included implicitly using the polarizable continuum model (PCM) with the parameters for THF.[42] Transition states and minima were confirmed through frequency calculations (no imaginary frequencies for minima, one imaginary frequency for transition states). Single point energies were computed with the pc-2[43] basis set. All Gibbs free energies are given at 298.15 K and 1 atm. The theoretically predicted *e.r.* was determined using a modified version of the Eyring equation (see equation in SI).[38,44]

Acknowledgements

This work was supported by the Research Council of Norway (No. 300769 and 313462), Sigma2 (No. nn9330k and nn4654k), the Nordforsk NordCO2 consortium (No. 85378) and UiT The Arctic University of Norway through funding of the iCCU-project.

References

[1] a) J. Davies, J. R. Lyonnet, D. P. Zimin, R. Martin, *Chem* **2021**, *7*, 2927–2942; b) A. Otto, T. Grube, S. Schiebahn, D. Stolten, *Energy Environ. Sci.* **2015**, *8*, 3283–3297.

[2] L. J. Gooßen, N. Rodríguez, K. Gooßen, *Angew. Chem. Int. Ed.* **2008**, *47*, 3100–3120.

[3] P. Ertl, E. Altmann, J. M. McKenna, *J. Med. Chem.* **2020**, *63*, 8408–8418.

[4] F. Calvo-Castañera, J. Álvarez-Rodríguez, N. Candela, Á. Maroto-Valiente, *Nanomaterials* **2021**, *11*, 190.

[5] a) R. Cauwenbergh, V. Goyal, R. Maiti, K. Natte, S. Das, *Chem. Soc. Rev.* **2022**, *51*, 9371–9423; b) X.-F. Liu, K. Zhang, L. Tao, X.-B. Lu, W.-Z. Zhang, *Green Chem.* **2022**, *3*, 125–137; c) A. Tortajada, F. Juliá-Hernández, M. Börjesson, T. Moragas, R. Martin, *Angew. Chem. Int. Ed.* **2018**, *57*, 15948–15982.

[6] a) F. Yan, J.-F. Bai, Y. Li, in *The Chemical Transformations of C1 Compounds*, John Wiley & Sons, Ltd, **2022**, pp. 1265–1303; b) Y. Shi, B.-W. Pan, Y. Zhou, J. Zhou, Y.-L. Liu, F. Zhou, *Org. Biomol. Chem.* **2020**, *18*, 8597–8619; c) C.-K. Ran, X.-W. Chen, Y.-Y. Gui, J. Liu, L. Song, K. Ren, D.-G. Yu, *Science China Chemistry* **2020**, *63*, 1336–1351; d) J. Vaitla, Y. Guttormsen, J. K. Mannisto, A. Nova, T. Repo, A. Bayer, K. H. Hopmann, *ACS Catal.* **2017**, *7*, 7231–7244.

[7] M. Takimoto, Y. Nakamura, K. Kimura, M. Mori, *J. Am. Chem. Soc.* **2004**, *126*, 5956–5957.

[8] S. Kawashima, K. Aikawa, K. Mikami, *Eur. J. Org. Chem.* **2016**, *2016*, 3166–3170.

[9] Y.-Y. Gui, N. Hu, X.-W. Chen, L. L. Liao, T. Ju, J.-H. Ye, Z. Zhang, J. Li, D.-G. Yu, *J. Am. Chem. Soc.* **2017**, *139*, 17011–17014.

[10] X.-W. Chen, L. Zhu, Y.-Y. Gui, K. Jing, Y.-X. Jiang, Z.-Y. Bo, Y. Lan, J. Li, D.-G. Yu, *J. Am. Chem. Soc.* **2019**, *141*, 18825–18835.

[11] J. Qiu, S. Gao, C. Li, L. Zhang, Z. Wang, X. Wang, K. Ding, *Chem. Eur. J.* **2019**, *25*, 13874–13878.

[12] L. Dian, D. S. Müller, I. Marek, *Angew. Chem. Int. Ed.* **2017**, *56*, 6783–6787.

[13] A. Cerveri, R. Giovanelli, D. Sella, R. Pedrazzani, M. Monari, O. Nieto Faza, C. S. López, M. Bandini, *Chem. Eur. J.* **2021**, *27*, 7657–7662.

[14] X.-W. Chen, J.-P. Yue, K. Wang, Y.-Y. Gui, Y.-N. Niu, J. Liu, C.-K. Ran, W. Kong, W.-J. Zhou, D.-G. Yu, *Angew. Chem. Int. Ed.* **2021**, *60*, 14068–14075.

[15] K. Zhang, H. Wang, S.-F. Zhao, D.-F. Niu, J.-X. Lu, *J. Electroanal. Chem.* **2009**, *630*, 35–41.

[16] Y.-J. Zhao, L.-R. Yang, L.-T. Wang, Y. Wang, J.-X. Lu, H. Wang, *Catal. Sci. Technol.* **2022**, *12*, 2887–2893.

[17] H.-P. Yang, Y.-N. Yue, Q.-L. Sun, Q. Feng, H. Wang, J.-X. Lu, *Chem. Commun.* **2015**, *51*, 12216–12219.

[18] B.-L. Chen, H.-W. Zhu, Y. Xiao, Q.-L. Sun, H. Wang, J.-X. Lu, *Electrochem. Commun.* **2014**, *42*, 55–59.

[19] K.-J. Jiao, Z.-M. Li, X.-T. Xu, L.-P. Zhang, Y.-Q. Li, K. Zhang, T.-S. Mei, *Org. Chem. Front.* **2018**, *5*, 2244–2248.

[20] L. Zhang, J. Cheng, B. Carry, Z. Hou, *J. Am. Chem. Soc.* **2012**, *134*, 14314–14317.

[21] a) S. W. Knowlden, PhD thesis thesis, West Virginia University **2022**; b) T. M. Perrone, A. S. Gregory, S. W. Knowlden, N. R. Ziemer, R. N. Alsulami, J. L. Petersen, B. V. Popp, *ChemCatChem* **2019**, *11*, 5814–5820; c) T. W. Butcher, E. J. McClain, T. G. Hamilton, T. M. Perrone, K. M. Kroner, G. C. Donohoe, N. G. Akhmedov, J. L. Petersen, B. V. Popp, *Org. Lett.* **2016**, *18*, 6428–6431.

[22] S. W. Knowlden, B. V. Popp, *Organometallics* **2022**, *41*, 1883–1891.

[23] Y.-Y. Gui, X.-W. Chen, X.-Y. Mo, J.-P. Yue, R. Yuan, Y. Liu, L.-L. Liao, J.-H. Ye, D.-G. Yu, *J. Am. Chem. Soc.* **2024**, *146*, 2919–2927.
[24] S. Zhang, L. Li, D. Li, Y.-Y. Zhou, Y. Tang, *J. Am. Chem. Soc.* **2024**, *146*, 2888–2894.
[25] a) S. Lin, Z. Lin, *Organometallics* **2019**, *38*, 240–247; b) X. Lv, Y.-B. Wu, G. Lu, *Catal. Sci. Technol.* **2017**, *7*, 5049–5054.
[26] N. N. Baughman, N. G. Akhmedov, J. L. Petersen, B. V. Popp, *Organometallics* **2021**, *40*, 23–37.
[27] T. Imamoto, K. Tamura, Z. Zhang, Y. Horiuchi, M. Sugiya, K. Yoshida, A. Yanagisawa, I. D. Gridnev, *J. Am. Chem. Soc.* **2012**, *134*, 1754–1769.
[28] J. Lee, S. Radomkit, S. Torker, J. del Pozo, A. H. Hoveyda, *Nat. Chem.* **2018**, *10*, 99–108.
[29] P.-A. Nocquet, T. Opatz, *Eur. J. Org. Chem.* **2016**, *2016*, 1156–1164.
[30] E. Bellur Atici, Ç. Ağtaş, Y. Yazar, N. Rıdvanoğlu, *J. Pharm. Biomed. Anal.* **2020**, *183*, 113145.
[31] S. Dei, C. Bellucci, C. Ghelardini, M. N. Romanelli, S. Spampinato, *Life Sci.* **1996**, *58*, 2147–2153.
[32] a) C. Pubill-Ulldemolins, A. Bonet, C. Bo, H. Gulyás, E. Fernández, *Chem. Eur. J.* **2012**, *18*, 1121–1126; b) K. Takahashi, T. Ishiyama, N. Miyaura, *J. Organomet. Chem.* **2001**, *625*, 47–53.
[33] a) X. Lv, Y.-B. Wu, G. Lu, *Catal. Sci. Technol.* **2017**, *7*, 5049–5054; b) L. Dang, H. Zhao, Z. Lin, T. B. Marder, *Organometallics* **2007**, *26*, 2824–2832.
[34] H. Ryu, J. Park, H. K. Kim, J. Y. Park, S.-T. Kim, M.-H. Baik, *Organometallics* **2018**, *37*, 3228–3239.
[35] a) J. I. Seeman, *J. Chem. Educ.* **1986**, *63*; b) J. I. Seeman, *Chem. Rev.* **1983**, *83*, 83–134.
[36] a) A. P. Deziel, S. Gahlawat, N. Hazari, K. H. Hopmann, B. Q. Mercado, *Chem. Sci.* **2023**, *14*, 8164–8179; b) A. P. Deziel, M. R. Espinosa, L. Pavlovic, D. J. Charboneau, N. Hazari, K. H. Hopmann, B. Q. Mercado, *Chem. Sci.* **2022**, *13*, 2391–2404; c) L. Pavlovic, M. Pettersen, A. Gevorgyan, J. Vaitla, A. Bayer, K. H. Hopmann, *Eur. J. Org. Chem.* **2021**, *2021*, 663–670; d) M. F. Obst, A. Gevorgyan, A. Bayer, K. H. Hopmann, *Organometallics* **2020**, *39*, 1545–1552; e) D. García-López, L. Pavlovic, K. H. Hopmann, *Organometallics* **2020**, *39*, 1339–1347; f) M. Obst, L. Pavlovic, K. H. Hopmann, *J. Organomet. Chem.* **2018**, *864*, 115–127; g) L. Pavlovic, J. Vaitla, A. Bayer, K. H. Hopmann, *Organometallics* **2018**, *37*, 941–948.
[37] An intramolecular step implies that the number of atoms between reactant and TS does not change, and the computational approximations employed to compute both states are similar, with potential errors largely cancelling out. A bimolecular step implies computations of two separate reactant species forming one TS, which implies a change in the number of atoms, basis functions, the solvation cavity and so forth, with potential errors not cancelling out to the same extent. We also note that computations of bimolecular reactions are done under standard state conditions (assuming that the reacting species are present 1:1), giving standard state energies, whereas the experimental rates (and the corresponding barriers) will be affected by the actual concentrations, which are not known for all components.
[38] M. J. Frisch, G. W. Trucks, H. B. Schlegel, G. E. Scuseria, M. A. Robb, J. R. Cheeseman, G. Scalmani, V. Barone, G. A. Petersson, H. Nakatsuji, X. Li, M. Caricato, A. V. Marenich, J. Bloino, B. G. Janesko, R. Gomperts, B. Mennucci, H. P. Hratchian, J. V. Ortiz, A. F. Izmaylov, J. L. Sonnenberg, Williams, F. Ding, F. Lipparini, F. Egidi, J. Goings, B. Peng, A. Petrone, T. Henderson, D. Ranasinghe, V. G. Zakrzewski, J. Gao, N. Rega, G. Zheng, W. Liang, M. Hada, M. Ehara, K. Toyota, R. Fukuda, J. Hasegawa, M. Ishida, T. Nakajima, Y. Honda, O. Kitao, H. Nakai, T. Vreven, K. Throssell, J. A. Montgomery Jr., J. E. Peralta, F. Ogliaro, M. J. Bearpark, J. J. Heyd, E. N. Brothers, K. N. Kudin, V. N. Staroverov, T. A. Keith, R. Kobayashi, J. Normand, K. Raghavachari, A. P. Rendell, J. C. Burant, S. S. Iyengar, J. Tomasi, M. Cossi, J. M. Millam, M. Klene, C. Adamo, R. Cammi, J. W. Ochterski, R. L. Martin, K. Morokuma, O. Farkas, J. B. Foresman, D. J. Fox, in *Gaussian 16 Rev. B.01*, Wallingford, CT, **2016**.
[39] J. P. Perdew, K. Burke, M. Ernzerhof, *Phys. Rev. Lett.* **1996**, *77*, 3865–3868.
[40] a) G. A. Petersson, M. A. Al-Laham, *J. Chem. Phys.* **1991**, *94*, 6081–6090; b) G. A. Petersson, A. Bennett, T. G. Tensfeldt, M. A. Al-Laham, W. A. Shirley, J. Mantzaris, *J. Chem. Phys.* **1988**, *89*, 2193–2218; c) T. Clark, J. Chandrasekhar, G. W. Spitznagel, P. V. R. Schleyer, *J. Comput. Chem.* **1983**, *4*, 294–301.
[41] S. Grimme, S. Ehrlich, L. Goerigk, *J. Comput. Chem.* **2011**, *32*, 1456–1465.
[42] J. Tomasi, B. Mennucci, R. Cammi, *Chem. Rev.* **2005**, *105*, 2999–3094.
[43] a) F. Jensen, *J. Chem. Phys.* **2013**, *138*, 014107; b) F. Jensen, *J. Phys. Chem. A* **2007**, *111*, 11198–11204; c) F. Jensen, T. Helgaker, *J. Chem. Phys.* **2004**, *121*, 3463–3470; d) F. Jensen, *J. Chem. Phys.* **2002**, *116*, 7372–7379; e) F. Jensen, *J. Chem. Phys.* **2001**, *115*, 9113–9125.
[44] Q. Peng, F. Duarte, R. S. Paton, *Chem. Soc. Rev.* **2016**, *45*, 6093–6107.